Evaluation of $Bi_2V_{0.9}Cu_{0.1}O_{5.35}$—an Aurivillius-Type Conducting Oxide—as a Cathode Material for Single-Chamber Solid-Oxide Fuel Cells

Zongping Shao[1]
Jennifer Mederos
Chan Kwak[2]
Sossina M. Haile[3]
e-mail: smhaile@caltech.edu

Materials Science,
California Institute of Technology,
Pasadena, CA 91125

The compound $Bi_2V_{0.9}Cu_{0.1}O_{5.35}$, a typical Aurivillius-type fast oxygen ion conductor, was evaluated as a possible cathode material for single-chamber solid-oxide fuel cells operated under mixed propane and oxygen. The material was found to be structurally stable under various $C_3H_8+O_2$ environments over a wide temperature range and furthermore displayed low catalytic activity for propane oxidation. However, at temperatures above 650°C, detrimental reactions between the cathode and the ceria electrolyte occurred, producing low conductivity interfacial phases. At these high temperatures the cathode additionally underwent extensive sintering and loss of porosity and, thus, stable fuel cell operation was limited to furnace temperatures of <600°C. Even under such conditions, however, the partial oxidation occurring at the anode (a ceria nickel cermet) resulted in cell temperatures as much as 70–110°C higher than the gas-phase temperature. This explains the sharp decrease in fuel cell performance with time during operation at a furnace temperature of 586°C. Under optimized conditions, a peak power density of ~60 mW/cm^2 was obtained, which does not compete with recent values obtained from higher activity cathodes. Thus, the poor electrochemical activity of $Bi_2V_{0.9}Cu_{0.1}O_{5.35}$, combined with its chemical instability at higher temperatures, discourages further consideration of this material as a cathode in single-chamber fuel cells.
[DOI: 10.1115/1.3182729]

1 Introduction

In recent years, single-chamber fuel cells (SCFCs) have received considerable attention in the portable power arena. The SCFC design, in which anode and cathode chambers are exposed to the same premixed fuel and oxidant gas stream [1–3], is inherently simple, offers superior resistance to mechanical and thermal shock, and enables quick start-up [4]. These characteristics, along with the compatibility of solid-oxide SCFCs with high energy density liquid fuels, are particularly attractive for the unique demands of portable power and can, for such applications, outweigh the drawbacks of low efficiencies.

Electrical power generation in SCFCs results from the selective catalytic activity of the anode and cathode materials toward the fuel-oxygen mixture; the cathode preferentially catalyzes the electroreduction in oxygen, whereas the anode preferentially catalyzes the partial oxidation of the fuel and the subsequent electrooxidation of the partial products [3]. The partial oxidation at the anode not only leads to low oxygen partial pressure at the anode surface but also generates locally the fuels (H_2 and possibly CO, though the latter may instead be consumed by the water gas shift reaction) that can be electrochemically oxidized for electrical power generation [5].

The principle of the SCFC operation introduces particularly demanding performance requirements of the cathode materials. In addition to the high oxygen reduction rate and conductivity required for traditional dual-chamber fuel cells, the cathode must also display low activity for the fuel oxidation and good chemical stability under the fuel-oxygen atmosphere. In recent years, several candidate materials have been examined including Au, $La_{1-x}Sr_xMnO_{3-\delta}$ (LSM), and $Sm_{0.5}Sr_{0.5}CoO_{3-\delta}$ (SSC) [3] with fuel cells incorporating $Ba_{0.5}Sr_{0.5}Co_{0.8}Fe_{0.2}O_{3-\delta}$ (BSCF) into composite cathodes yielding particularly high power outputs [6,7]. The characteristics of BSCF suggest that oxides with high oxygen diffusivity may be well suited as SCFC cathodes. Accordingly, in this work we present an investigation of a typical $BiMeVO_x$ oxide, i.e., $Bi_2V_{0.9}Cu_{0.1}O_{5.35}$, a fast oxide ion conducting Aurivillius phase, as a possible cathode material for single-chamber fuel cells operated on $C_3H_8+O_2+He$ gas mixtures.

Aurivillius phase materials, first reported by Aurivillius in 1950 [8–10], are based on a layered bismuth oxide/perovskite structure. The stoichiometry of such phases is generally formulated as $Bi_2A_{n-1}B_nO_{3n+3}$ (A=Na, K, Ca, Sr, Ba, etc., and B=V, Fe, Cr, Ti, Ga, Nb, Mo, W, etc.), and the structures consist of n perovskite-like layers $(A_{n-1}B_nO_{3n+1})^{2+}$ (n=1–5) sandwiched between bismuth-oxygen sheets $(Bi_2O_2)^{2+}$. The end-member $Bi_2VO_{5.5}$ (or $Bi_4V_2O_{11}$) is a single-layer Aurivillius phase in which 1/8 of the oxygen sites of the perovskite layer are vacant (i.e., $(Bi_2O_2)^{2+}(VO_{3.5}\square_{0.5})^{2-}$). At high temperatures, above ~570°C, the vacancies are highly mobile and disordered and the material adopts a tetragonal structure (the γ-phase), which has exceptionally high oxide ion conductivity: 0.1–1 S cm^{-1} at 600°C [11,12]. Intro-

[1]Present address: College of Chemistry and Chemical Engineering, Nanjing University of Technology, PR China.
[2]Present address: Samsung SDI, Corp. R&D, Shin Dong 575, Gyeonggi Do 443731, South Korea.
[3]Corresponding author.
Manuscript received May 8, 2008; final manuscript received February 3, 2009; published online January 12, 2010. Review conducted by Ellen Ivers-Tiffée.

duction of dopants onto the vanadium site can stabilize the highly conductive γ-phase to low temperatures, and the series of compounds so modified, with stoichiometry $Bi_2V_{1-x}Me_xO_{5.5-\delta}$, are generally referred to as the $BiMeVO_x$ family [13]. Within this group, the highest conductivities have been measured in γ-phase Bi–V–Cu–O, Bi–V–Ni–O, and Bi–V–Sb–O materials, which exhibit oxygen ionic conductivities two orders of magnitude higher than any other known oxygen ionic conductor in the temperature range 300–500°C [12,14]. In particular, $Bi_2V_{0.9}Cu_{0.1}O_{5.35}$ has an oxygen ionic conductivity of 5×10^{-2} S cm^{-1} at 500°C [13].

For solid-oxide fuel cell (SOFC) cathode applications, in addition to high ionic conductivity, high catalytic activity and high electronic conductivity are essential. However, $BiMeVO_x$ materials typically display measurable electronic transport only under moderately reducing atmospheres ($pO_2 < \sim 10^{-5}$ atm) [15]. To address this shortcoming, it is possible to utilize the fast ion conductor in conjunction with an electronically conducting second phase, i.e., in composite form with a metal such as silver. Indeed, such an approach was already reported in the literature with $Bi_2V_{0.9}Cu_{0.1}O_{5.35}$(50 vol %)+Ag(50 vol %) being implemented as a composite cathode material in dual-chamber fuel cells. Using thin-film samaria doped ceria (SDC) as the electrolyte and SDC +Ni as the anode, impressive peak power densities of 130 mW/cm^2, 231 mW/cm^2, and 443 mW/cm^2 were reported at 450°C, 500°C, and 550°C, respectively [16]. The results suggest that, in addition to sufficient electronic and ionic conductivity, the composite system also exhibits high catalytic activity for oxygen electroreduction and motivate the present examination of $Bi_2V_{0.9}Cu_{0.1}O_{5.35}$ as a potential cathode in single-chamber SOFCs (SC-SOFCs).

2 Experimental

2.1 Powder Synthesis. The target material $Bi_2V_{0.9}Cu_{0.1}O_{5.35}$ was synthesized by a solution route to ensure chemical homogeneity, using a combined ethylene diamine tetraacetic acid (EDTA)-citrate complexing method [17]. Stoichiometric amounts of $Bi(NO_3)_3\cdot6H_2O$ (Alfa Aesar (Ward Hill, MA), >98%), NH_4VO_3 (Alfa Aesar, >99%), and $Cu(NO_3)\cdot5H_2O$ (Alfa Aesar, >98%) were first mixed with a citric acid solution to form a yellow suspension. An EDTA-ammonia solution was then added while stirring and heating to yield a dark blue transparent solution. The mole ratio of citric acid:EDTA acid:total metal ions was set to 2:0.5:1. The water in the solution was slowly evaporated at 80°C under stirring to yield a blue gel, which was then fired at 250°C for 10 h and subsequently calcined at 500°C for 24 h and at 700°C for 5 h to form the $BiMeVO_x$ phase. Both the as-prepared powder and samples exposed to various conditions relevant to single-chamber fuel cell operation, as described below, were examined by X-ray powder diffraction (Philips X-pert Pro, Cu $K\alpha$, $\lambda=1.5408$ Å). In addition, the possible reaction between the cathode and electrolyte materials was evaluated by firing 50:50 wt % mixtures of SDC and $Bi_2V_{0.9}Cu_{0.1}O_{5.35}$ (combined by light milling) at temperatures between 500°C and 850°C for 6 h under air.

2.2 Characterization of Catalytic Activity. Ideally, the cathode for a SCFC should only catalyze the oxygen reduction process, but often mixed conducting oxides show measurable activity for hydrocarbon oxidation. The catalytic activity of the $Bi_2V_{0.9}Cu_{0.1}O_{5.35}$ oxide was evaluated using a vertically oriented, flow-through quartz tube reactor with an inner diameter of approximately 6 mm. The catalyst bed consisted of ~0.3 g powder mixed with 1.5 g inert quartz sand (100–120 mesh) to minimize the temperature inhomogeneity within the bed. The inlet gas was composed of propane+oxygen+helium supplied at rates of 1 ml/min, 5 ml/min, and 120 ml/min, respectively. The propane-to-oxygen ratio of 1:5 used for these experiments corresponds precisely to that for complete oxidation of propane (to CO_2 and H_2O), providing a stringent test for the absence of catalytic activity. Helium rather than nitrogen, the latter of which would be the inert gas of choice because of its ready availability, was used to facilitate analysis of the off-gas composition; the micro gas chromatograph (GC) signal of N_2 overlaps with that of O_2 at high concentrations. The effluent gas from the reactor was directed to a Varian CP 4900 micro gas chromatograph for on-line composition analysis. A capillary Propak Q column was used for the separation of air+CO, CH_4, CO_2, C_2H_4, C_2H_6, H_2O, C_3H_6, and C_3H_8, and a molecular sieve 5A capillary column was used for the separation of H_2, O_2, N_2, CH_4, and CO. Conversions of C_3H_8 and O_2 were calculated based on the carbon and oxygen balances, respectively.

2.3 Fuel Cell Fabrication and Characterization. For the electrolyte and anode components of the fuel cell, respectively, thin-film SDC15 ($Sm_{0.15}Ce_{0.85}O_{1.925}$) and Ni+SDC15 were selected because of the high oxygen ionic conductivity of SDC at moderate temperatures and the good catalytic activity of Ni for propane partial oxidation [18]. The anode was prepared from a mixture of SDC (either obtained from NexTech Materials (Lewis Center, OH), or synthesized in-house by solid state reaction of the component oxides) and nickel oxide (Alfa Aesar) combined in a weight ratio of 40:60 and ball milled for 12 h. To this powder mix, PVP8000 (polyvinylpyrrolidone, molecular weight of 8000, Alfa Aesar) dissolved in water was added as a fugitive pore-former. After drying and grinding, the mixture was passed through a 200-mesh sieve, and then pressed into pellets. To obtain an anode-electrolyte bilayer, a thin SDC15 layer was applied to the pellet by a dual dry-pressing process, described in detail elsewhere [18]. The bilayer structure was sintered at 1350°C under air for 5 h to densify the ~20 μm SDC thin layer and remove the organic pore-former. The sample was then treated under flowing hydrogen atmosphere at 600°C for 5 h to reduce the NiO in the anode to Ni. The cathode powder $Bi_2V_{0.9}Cu_{0.1}O_{5.35}$ was applied to the bilayer by first mixing it with Ag powder at a volume ratio of 50:50 (to obtain the requisite electronic conductivity). The mixture was deposited onto the electrolyte surface of the anode-supported bilayer by spraying, using an isopropyl alcohol-based liquid media. The complete fuel cell structure was then fired at 600°C under nitrogen atmosphere for 5–6 h. The firing temperature was kept relatively low because of the low melting temperatures of the components in the cathode mixture (~825°C for $Bi_2V_{0.9}Cu_{0.1}O_{5.35}$ and 962°C for Ag), while the inert atmosphere was required to simultaneously retain the Ni of the anode in the reduced state and the $Bi_2V_{0.9}Cu_{0.1}O_{5.35}$ in the cathode in the oxidized state. The disk shaped fuel cells had a final diameter of 13.3 mm, an anode porosity of ~50% and thickness of ~0.7 mm, an electrolyte thickness between 10 μm and 40 μm, and a cathode thickness of roughly 10 μm.

The surface morphology of the fuel cells and cathodes was examined by high-resolution scanning electron microscopy using a LEO 1550 VP field emission SEM equipped with an Oxford energy dispersive spectrometer (EDS) for chemical analysis. Structural changes that might be induced by high temperature exposure during fuel cell operation were probed by microstructural observation of complete membrane-electrode-assemblies fired at 650°C, 700°C, and 800°C (6 h, air atmosphere).

To enable electrical measurements, contacts were made to the fuel cell as follows. Gold wires were first attached to small pieces of silver gauze (~0.2 cm^2, Alfa Aesar), which were then affixed to the electrode surfaces using silver conductive ink (Alfa Aesar). Satisfactory adhesion to the electrodes was attained after drying under an IR lamp (~120°C) for 15 min. In order to ensure sufficient electrical conductivity for the cathode, an additional thin layer of colloidal silver paste (Ted Pella, Inc., Redding, CA) was applied (and dried for 5 min). Fuel cell polarization curves were measured in galvanostatic mode using a Keithley 2420 sourcemeter with a maximum current output of 3 A and a dc voltage output of 60 V. The instrument was interfaced with a computer and controlled through a program written using LABVIEW 6.1 soft-

ware. Data were obtained using a four-probe technique to eliminate the effect of the wire resistances, and power densities were calculated based on the cathode surface area (which was typically 0.71 cm^2 as compared with 1.39 cm^2 for the electrolyte).

The gas supply to the fuel cells during polarization measurement was controlled using the same flow-through test-station employed for catalysis measurements but with a larger reactor (an inner diameter of 1.59 cm). The premixed gas stream was supplied through the top of the reactor and the cells were placed parallel to the streamwise direction. The fuel cell temperature, which is well-documented to rise as much as 150°C above that of the furnace or gas-phase temperature as a consequence of in situ oxidation reactions at the anode [7], was monitored using a K-type thermocouple placed in contact with the center of the anode side of the membrane-electrode assembly (MEA). Polarization measurements were performed at furnace temperatures of 475–625°C with an inlet gas typically composed of propane +oxygen+helium supplied at rates of 10 ml/min, 24–36 ml/min, and 120–180 ml/min, respectively. The O_2:He volumetric ratio was maintained at approximately 1:4 in order to simulate the oxygen content of air. With this set of gas flow rates, the O_2:C_3H_8 ratio was varied from 2.4 to 3.6, corresponding to compositions that were 2.08 to 1.38 times rich in propane relative to the stoichiometric ratio for complete oxidation. It was generally observed [18] that optimal power output from single-chamber fuel cells is obtained at oxygen-to-fuel ratios intermediate between those required for complete and for partial oxidation [3,7] (5 and 1.5, respectively, for propane), predicating this choice of gas mixtures for examination. Under such fuel rich conditions, however, carbon deposition can become problematic. The possibility of carbon coking was evaluated by thermodynamic calculations using the commercial software package HSC CHEMISTRY (Version 5.1, Outokumpu Research Oy, Finland).

3 Results

3.1 Phase Stability Under Single-Chamber Configuration. The X-ray powder diffraction patterns obtained from $Bi_2V_{0.9}Cu_{0.1}O_{5.35}$ after treatment under various experimental conditions are presented in Fig. 1. The pattern in Fig. 1(*a*) is that obtained immediately after synthesis. All observed peaks can be attributed to the γ' modification of $BiMeVO_x$, an incommensurate superstructure of the γ-phase with partially ordered oxygen ions [13]. The result agrees with the well-established observation in the literature that $BiMeVO_x$ exists stably as the γ'-type phase at temperatures below 450–500°C [19]. Upon heating, the γ'-phase is reported to revert to the fully disordered γ-phase [20], and thus at the operating temperatures in our fuel cell experiments, >500°C, $Bi_2V_{0.9}Cu_{0.1}O_{5.35}$ is expected to exist in the high conductivity γ-phase.

Figure 1(*b*) shows the diffraction patterns of the $Bi_2V_{0.9}Cu_{0.1}O_{5.35}$ after exposure to a flowing propane-oxygen-helium stream (10 SCCM C_3H_8+20 SCCM O_2+120 SCCM He (SCCM denotes cubic centimeter per minute at STP)) at temperatures between 500°C and 700°C for 6 h (data collected post situ). No additional peaks beyond those of the original γ'-phase were detected, indicating that $Bi_2V_{0.9}Cu_{0.1}O_{5.35}$ is stable under the propane-oxygen-helium mixtures investigated for single-chamber fuel cell operation. On increasing the propane content in the gas stream, the $Bi_2V_{0.9}Cu_{0.1}O_{5.35}$ maintained structural stability even at a 5:1 methane:O_2 ratio (see Fig. 1(*c*)). Under neat propane and at high temperatures (T=700°C, t=6 h), however, the $Bi_2V_{0.9}Cu_{0.1}O_{5.35}$ was found to be partially decomposed. A minor amount of elemental copper was detected, and the Cu-depleted $Bi_2V_{0.9}Cu_{0.1}O_{5.35}$ formed a $Bi_6V_3O_{16}$ phase (JCPDPS File Card No. 86-0392) in addition to at least one other unidentified phase. Though not directly relevant to SCFC operation here, it is noteworthy that this decomposition was not observed for lower temperature and shorter time exposure to propane (e.g., 5 h at

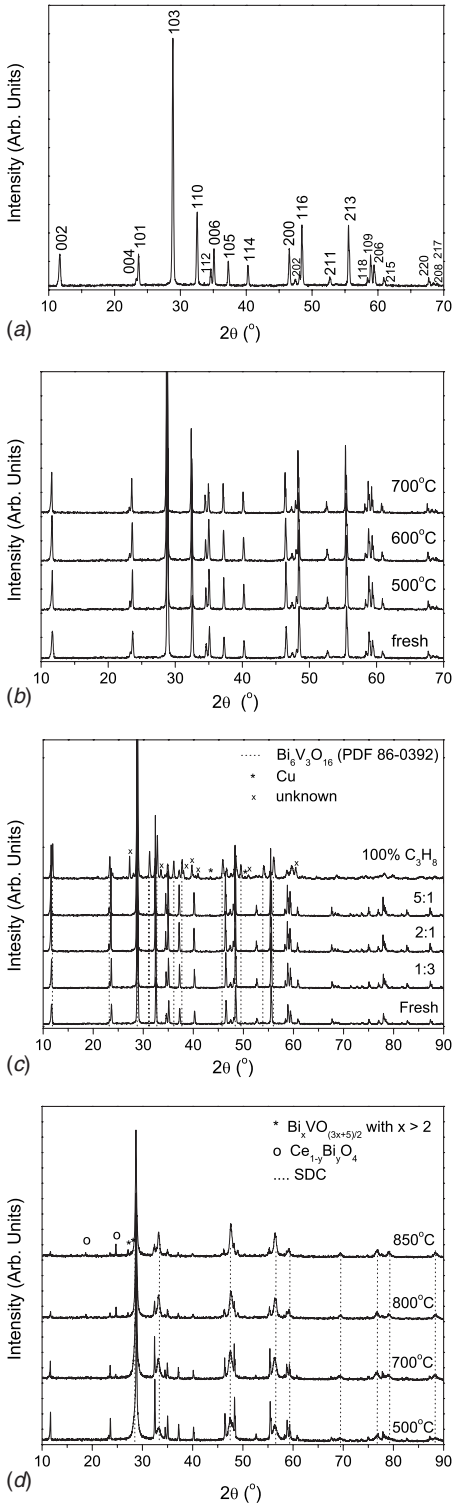

Fig. 1 X-ray diffraction patterns of $Bi_2V_{0.9}Cu_{0.1}O_{5.35}$ oxide (obtained from the EDTA-complexing method) after treatment under various conditions: (*a*) after calcination at 700°C for 6 h in air; (*b*) powder (*a*) after 6 h exposure to 10 ml/min C_3H_8 +30 ml/min O_2+120 ml/min He at the temperatures indicated; (*c*) powder (*a*) after 6 h exposure at 700°C to a gas stream with the propane-to-oxygen ratio as indicated and fixed propane and helium flow rates of 10 ml/min and 120 ml/min, respectively; and (*d*) mixtures of 50 wt % SDC+50 wt % $Bi_2V_{0.9}Cu_{0.1}O_{5.35}$ after a 6 h anneal under air at the temperatures indicated

500°C). Overall, the diffraction study reveals that $Bi_2V_{0.9}Cu_{0.1}O_{5.35}$ is stable against reduction or other phase transformation under the typical propane+oxygen atmospheres of a single-chamber fuel cell.

Figure 1(*d*) shows the X-ray diffraction patterns of mixtures of SDC15 and $Bi_2V_{0.9}Cu_{0.1}O_{5.35}$ after exposure to selected temperatures. All the diffraction peaks for the sample annealed at 500°C can be attributed to either SDC15 or $Bi_2V_{0.9}Cu_{0.1}O_{5.35}$, indicating negligible reactivity between the two components at moderate temperatures. At 700°C and higher, however, secondary phases began to appear with the extent of reaction increasing strongly with temperature. These secondary phases are identified as $Bi_xVO(3x+5)/2$ $(x>2)$ and $Ce_{1-y}Bi_yVO_4$ zircon-type materials. The compounds $Bi_xVO(3x+5)/2$ $(x>2)$, though primarily oxide ion conductors, have ionic conductivities many times lower than that of $Bi_2V_{0.9}Cu_{0.1}O_{5.35}$ [21–26], whereas $Ce_{1-y}Bi_yVO_4$ exhibits primarily electronic transport, but again, with low conductivity [27] (five to ten times lower than that of γ-phase $Bi_2V_{0.9}Cu_{0.1}O_{5.35}$). The undesirable properties of these product phases suggest that fuel cell performance will degrade upon reaction of SDC15 with $Bi_2V_{0.9}Cu_{0.1}O_{5.35}$.

3.2 Catalytic Activity for Propane Oxidation. The catalytic activity of $Bi_2V_{0.9}Cu_{0.1}O_{5.35}$ in powder form for propane oxidation is presented in Fig. 2 along with analogous results for a purely gas-phase reaction (as measured in the blank reactor). It is apparent that $Bi_2V_{0.9}Cu_{0.1}O_{5.35}$ has very poor activity for propane oxidation, with propane and oxygen conversion rates barely exceeding those of the blank reactor (see Fig. 2(*a*)). In both cases, with and without $Bi_2V_{0.9}Cu_{0.1}O_{5.35}$, measurable reactivity occurs only at temperatures above approximately 600°C. At these high temperatures, the gas-phase reaction primarily consists of thermal cracking of C_3H_8 to yield C_2H_2 and CH_4, and oxidative dehydrogenation of C_3H_8 to yield C_3H_6. Along with a slight increase in overall C_3H_8 and O_2 conversion rates, as compared with the blank reactor, a slight suppression of C_3H_8 and CH_4 and a slight enhancement of the oxidation products CO_2 and CO occur in the presence of $Bi_2V_{0.9}Cu_{0.1}O_{5.35}$. This observation suggests that the oxide plays a role in redirecting oxygen away from oxidative dehydrogenation (of C_3H_8 to C_3H_6) and toward oxidation of CH_4 to CO, CO_2, and H_2O with a very limited impact on the thermal cracking behavior. While an influence of $Bi_2V_{0.9}Cu_{0.1}O_{5.35}$ on propane oxidation is detectable above ~650°C, the overall activity of this material for catalytic propane oxidation is low, as is necessary for implementation as a cathode in single-chamber solid-oxide fuel cells. Indeed, the activity in this regard is even lower than that of $Sr_{0.5}Sm_{0.5}CoO_{3-\delta}$ [18] and $Ba_{0.5}Sr_{0.5}Co_{0.8}Fe_{0.2}O_{3-\delta}$ [6], cathode materials with good-to-excellent performance in single-chamber fuel cells.

The low catalytic activity of $Bi_2V_{0.9}Cu_{0.1}O_{5.35}$ for propane oxidation is likely responsible, in part, for the phase stability of the oxide even under relatively high propane atmospheres up to moderate temperatures (see Fig. 3). Under such conditions, $Bi_2V_{0.9}Cu_{0.1}O_{5.35}$ simply does not interact with propane and thus the oxide retains its structural oxygen. The phase stability at even higher temperatures at which CO and H_2 are produced (primarily via gas-phase reaction) may be related to the high activity of $Bi_2V_{0.9}Cu_{0.1}O_{5.35}$ for oxygen electroreduction and the high oxide ion conductivity. Upon reduction in $Bi_2V_{0.9}Cu_{0.1}O_{5.35}$ by these species, rapid oxygen incorporation to the surface from the gas phase followed by diffusion into the structure may mitigate the occurrence of oxygen depleted regions that would favor phase degradation. Despite the stability of $Bi_2V_{0.9}Cu_{0.1}O_{5.35}$ to relatively high temperatures under relatively high propane concentrations, the onset of extensive gas-phase reactions at high temperatures limits propane fueled single-chamber fuel cells to operational temperatures of less than ~650°C, irrespective of cathode material [18].

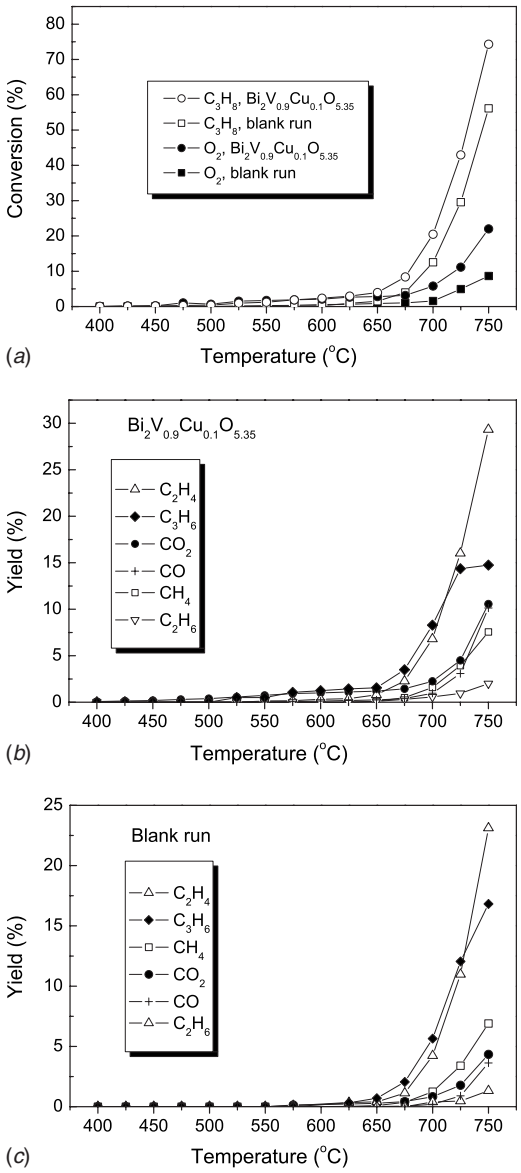

Fig. 2 The temperature dependence of the catalytic activity of $Bi_2V_{0.9}Cu_{0.1}O_{5.35}$ for propane oxidation, as measured using 0.3 g of catalyst under C_3H_8:1 ml/min, O_2:5 ml/min, He:120 ml/min: (*a*) propane and oxygen conversion with and without the catalyst, (*b*) yield of carbon based products obtained over the catalyst, and (*c*) without the catalyst

3.3 Microstructural Stability. Figure 3 shows scanning electron micrographs (SEMs) of the as-prepared MEAs and the cathode surfaces after firing at various temperatures. After firing at 600°C (the default processing condition), the cathode displayed good attachment to the electrolyte layer and retained favorable porosity. With an increase in firing temperature, the cathode porosity decreased dramatically, becoming almost completely densified after processing at 700°C. Firing at 800°C caused even more severe changes; the $Bi_2V_{0.9}Cu_{0.1}O_{5.35}$ evaporated to such an extent that the remaining Ag and $BiVCuO_x$ could not cover the electrolyte surface. In light of the severe microstructural changes upon high temperature exposure, it is apparent that fuel cell operation temperatures must be maintained at values of 600°C or less.

3.4 Fuel Cell Performance. A first set of fuel cell experiments was performed in which the power output was measured as a function of time under a fixed set of environmental conditions.

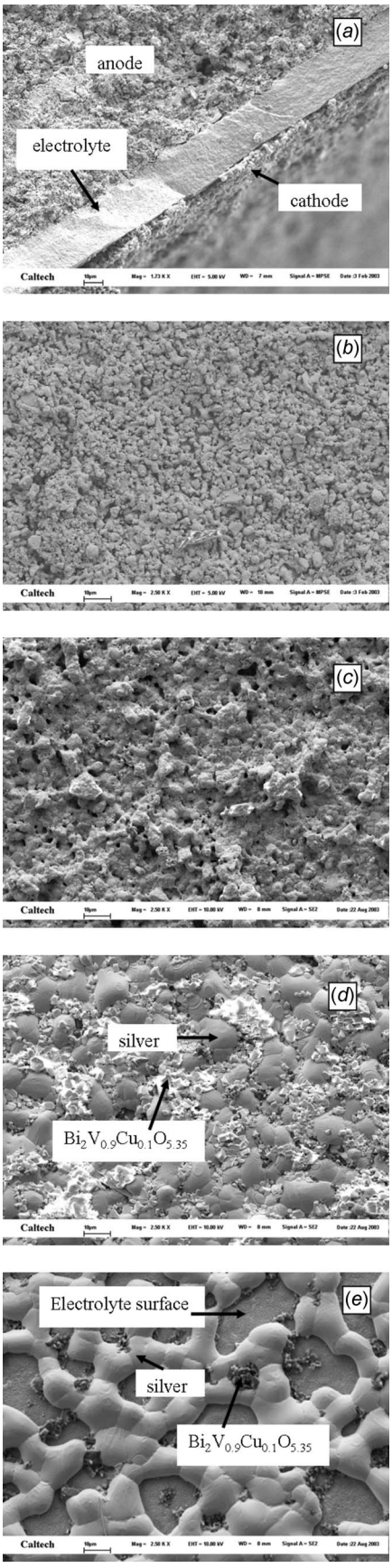

Fig. 3 Scanning electron micrographs showing (*a*) the cross section of the as-fabricated complete fuel cell (fired at 600°C, 6 h) and the surface morphologies of the cathode after firing for 6 h at (*b*) 600°C, (*c*) 650°C, (*d*) 700°C, and (*e*) 800°C

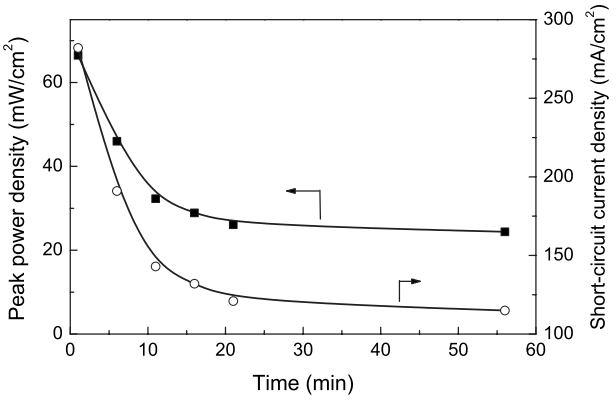

Fig. 4 Fuel cell performance as function of time for a gas stream temperature of 587°C under a gas stream of C_3H_8:10 ml/min, O_2:40 ml/min, and He:120 ml/min

Prior to exposure to the reactant gases, the fuel cell was heated to 587°C under flowing He atmosphere. Upon stabilization of the furnace temperature, the oxygen and propane were switched on for flow compositions of 120 SCCM He, 10 SCCM C_3H_8, and 40 SCCM O_2. After the open circuit voltage (OCV) reached a stable value (which occurred within approximately 1 min), the first polarization curve was collected, and then the measurement periodically repeated. Figure 4 shows the time on stream dependence of the fuel cell performance. Initially, the performance decreased quickly. Relatively stable performance was attained after about half an hour and power output appeared to have reached a fixed value by the end of the 1 h examination, although longer term tests may have shown continued gradual degradation. In contrast to the current output, the OCV was found to remain at about 0.65 V throughout the 1 h period. The decrease in fuel cell performance is accordingly attributable to an increase in internal resistance. In general, this type of degradation was not observed at lower temperatures, specifically, below operating temperatures of about 570°C.

A second set of experiments (using a fresh MEA) was performed in which the impact, at a given temperature, of the O_2:C_3H_8 ratio on power output was examined. The experiment was carried out at a furnace temperature of 514°C, at which power output does not degrade with time, and at lower oxygen flow rates than the first degradation study, which, as discussed below, is also important for minimizing thermal degradation. After an initial heating under helium (again, to 587°C), the reactant gases were introduced and the polarization data collected. For each set of gas conditions, the cell was equilibrated for approximately 5 min. The propane and helium gas flow rates were held constant at 10 ml/min and 120 ml/min, respectively, while the oxygen flow rate was varied between 24 ml/min and 38 ml/min. Within this range of conditions, it was found (see Fig. 5) that the OCV increased monotonically with oxygen flow rate, whereas the peak power density first rose then fell, displaying a maximum value of 24 mW/cm^2 at an oxygen flow rate of 32 ml/min.

In a third set of experiments (again, using a fresh MEA), the correlation between optimal fuel-to-oxygen ratio and temperature (over the range 475–625°C) was examined. As in the experiments described above, measurements were performed after an initial heating and 5 min annealing under Ar at 625°C. After this stabilization period, polarization data were acquired for the range of fuel mixtures (with the oxygen-to-propane ratio being swept from high to low) before purging with Ar and lowering to the next measurement temperature. Measurements were performed relatively quickly to minimize degradation effects. The peak power densities achieved using optimal oxygen-to-propane ratios at various temperatures are shown in Fig. 6. In general, the optimal oxygen-to-propane ratio increased with temperature, whereas the

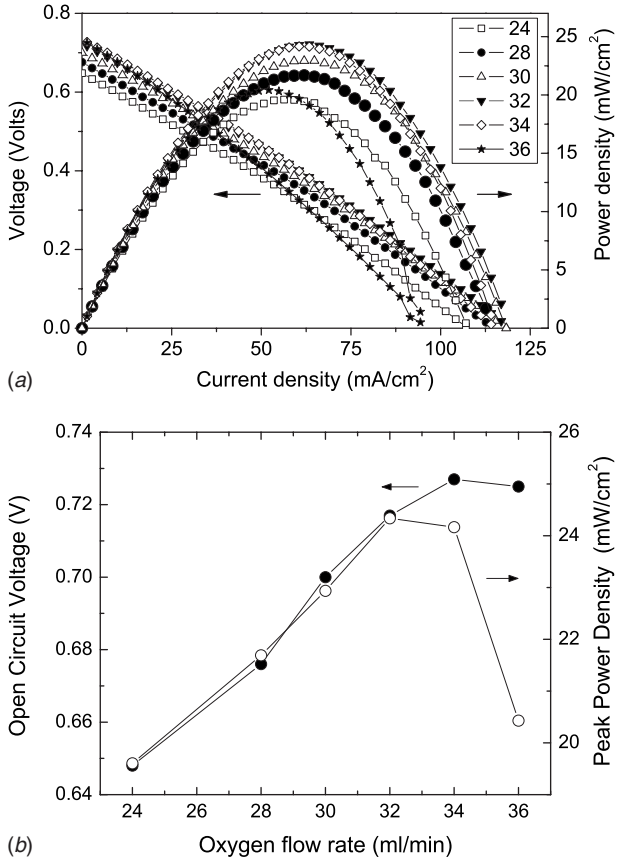

Fig. 5 The fuel cell performance at a gas-phase temperature of 514°C and a propane flow rate of C_3H_8:10 ml/min, an O_2 flow rate as indicated (24–36 ml/min), and a He flow rate five times that of the oxygen flow rate (120–180 ml/min): (*a*) polarization curves and (*b*) open circuit voltage and peak power density as functions of the oxygen flow rate

peak power density reached a maximum value of almost 60 mW/cm^2 at a furnace temperature of 562°C. In comparison to methane operated single-chamber fuel cells, the maximal power output occurs at somewhat low fuel-to-oxygen ratios, 1.23–1.38 rich in propane relative to the stoichiometric value for complete oxidation, whereas for methane the corresponding values are in the range 2.49–1.93 [7]. The difference may result from the higher hydrogen content of methane, which enables a greater portion of

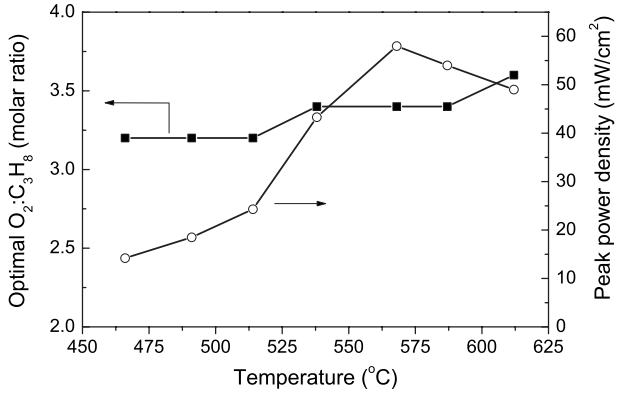

Fig. 6 Temperature dependence (gas-phase temperature) of the optimal oxygen-to-propane ratio at a constant propane flow rate of 10 ml/min and a helium flow rate five times that of the oxygen flow rate

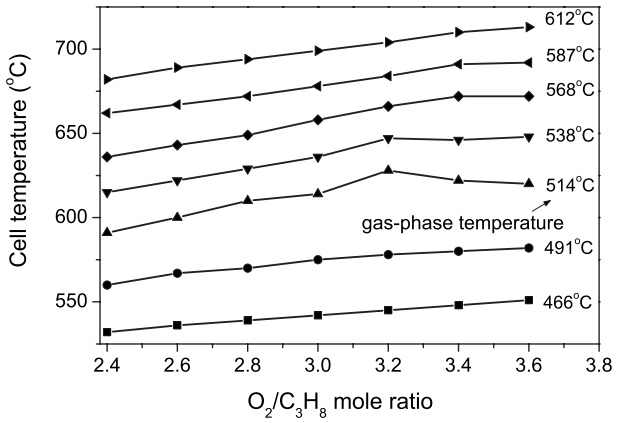

Fig. 7 Cell temperature (at open circuit) as a function of oxygen-to-propane molar ratio at selected gas stream temperatures. Propane flow rate fixed at 10 ml/min, oxygen flow rate varied from 24 ml/min to 36 ml/min, and helium flow rate set to five times that of the oxygen.

the fuel to utilized electrochemically, but certainly greater experimentation is required to provide a definitive explanation, as there are also differences in fuel cell temperature and cathode material choice in these studies.

Overall, the open circuit values achieved here, ~0.7 V (see Fig. 5) at a (gas phase) temperature of ~515°C, are comparable to the values attained using essentially identical cells but with cathodes comprised of either $(Ba_{0.5}Sr_{0.5})(Co_{0.8}Fe_{0.2})O_{3-\delta}$+SDC composites [4,6] or $(Sm_{0.5}Sr_{0.5})CoO_{3-\delta}$+SDC composites [18]. In contrast, the power outputs from $Bi_2V_{0.9}Cu_{0.1}O_{5.35}$ containing SCFCs are substantially lower than from those cells, which were reported to be as high as 440 mW/cm^2 [6] and 210 mW/cm^2 [18], respectively.

3.5 Fuel Cell Temperature. As already alluded to, the actual temperature at the anode of a single-chamber SOFC can be substantially higher than that of the surrounding gas stream, the latter being established by the temperature of the furnace. This effect is illustrated in Fig. 7 in which the measured cell temperature (at OCV) is reported as a function of the O_2:C_3H_8 ratio for selected furnace temperatures. The experimental conditions correspond to those of Fig. 6 (propane and helium flow rates fixed at 10 ml/min and 120 ml/min, respectively, and oxygen flow rate varied from 24 ml/min to 36 ml/min). It was found that the fuel cell temperature was 70–110°C higher than the gas-phase temperature under these conditions, with the differential increasing with an increase in gas flow rate. With fixed helium and propane flow rates, an increase in oxygen flow rate from 24 ml/min to 36 ml/min increased the differential by 20–30°C. Similarly, an increase in the propane flow rate to 40 SCCM resulted in a temperature differential of as much as 270°C under selected conditions (data not shown). In the particular case of the $Bi_2V_{0.9}Cu_{0.1}O_{5.35}$-based fuel cell operated at a gas-phase temperature of 587°C, and oxygen, propane, and helium flow rates of 40 ml/min, 10 ml/min, and 120 ml/min, respectively (see Fig. 4), the actual fuel cell temperature was, in fact, greater than 700°C. At such high temperatures, sintering and sublimation of the cathode occur, as discussed in Sec. 3.3, and are likely the causes of the observed degradation in fuel cell power output.

The fact that the anodes of single-chamber solid-oxide fuels are much hotter than the surrounding gas stream is now well-documented in the literature [3,7,18,28]. The phenomenon is a result of the (direct chemical) exothermic oxidation reactions that are catalyzed by the Ni in the anode. Not only does chemical oxidation release heat, it does so inhomogeneously across the surface of the anode. Specifically, because the MEA is placed parallel

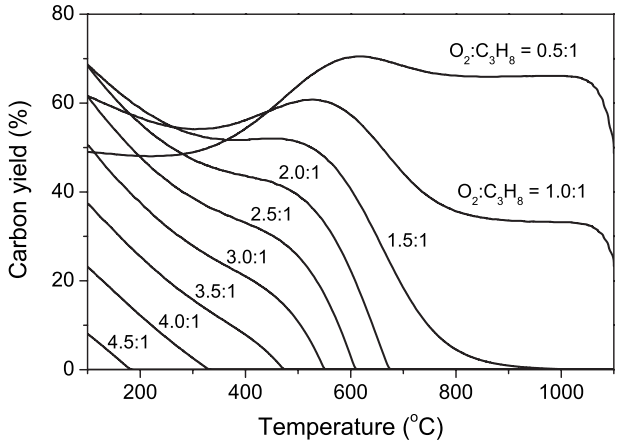

Fig. 8 Expected carbon yields under thermodynamic equilibrium for indicated oxygen-to-propane ratios in the feed gas

to the direction of gas flow, one edge of the cell is, by definition, the upstream or leading edge. Here, the gas stream makes first contact with the fuel cell, and this is indeed where most of the oxidation reactions can be expected to occur. Evaluation of the temperature gradient across the length (or diameter) of the cell using multiple thermocouples confirmed that the leading edge of the fuel cell was indeed as much as 50°C hotter than the trailing edge. The middle point of the fuel cell was taken as the average cell temperature.

3.6 Carbon Coking. Visual inspection of the MEAs after exposure to various gas streams revealed that the $Bi_2Vi_{0.9}Cu_{0.1}O_{5.35}$+Ag cathode did not catalyze carbon deposition at any relevant temperature. In contrast, the anode was susceptible to carbon coking. When the fuel cell was exposed to pure propane at high temperature (T=600°C), carbon deposits appeared almost immediately at the anode surface; cracks formed within 1 min and eventually the anode disintegrated into a loose powder. The presence of oxygen in the reactant stream helped suppress carbon coking at the anode surface. At oxygen-to-propane ratios of 3.0 and higher, no visible carbon coking occurred at temperatures above 500°C. Below 500°C, some carbon deposits were observed at low oxygen-to-propane ratios but only at the leading edge of the fuel cell anode. The thermodynamic conditions for carbon deposition are illustrated in Fig. 8 with carbon yield plotted as a function of temperature for several $O_2:C_3H_8$ ratios (with the helium-to-oxygen ratio fixed at 4:1 to reflect the experimental conditions). It can be seen that, thermodynamically, for an oxygen-to-propane ratio of <1.5, a considerable amount of carbon coking is expected, even at temperatures above 800°C. With increasing oxygen-to-propane ratio, the critical temperature for carbon coking (above which the computed carbon yield is essentially zero) decreases, from 675°C for $O_2:C_3H_8$=2.0:1 to 475°C for $O_2:C_3H_8$=3.5:1. These results suggest that the fuel cells operated at low to moderate temperatures should be supplied with a gas stream of relatively high oxygen-to-propane ratio. However, this requirement must be balanced against the need to operate at an optimal fuel-to-oxygen ratio with respect to electrical power output. Our tests demonstrated that the optimal oxygen-to-propane ratio is about 3.2:1, which means that the fuel cell should be operated at a temperature higher than 520°C in order to avoid carbon coking.

4 Discussion and Conclusions

Single-chamber fuel cells operate on the principle of selective catalysis. For operation on propane, the anode ideally catalyzes the partial oxidation reaction, given as

$$C_3H_8 + 1.5O_2 \rightarrow 3CO + 4H_2, \quad \Delta H = -227.78 \text{ kJ/mol at } 25\,^\circ\text{C}$$

and this highly exothermic reaction is responsible for the temperature rise at the fuel cell as discussed above. The H_2 and, to some extent, CO generated at the anode can then participate in electrochemical oxidation (while oxygen is electrochemically reduced at the cathode) to produce electrical power. The ideal oxygen-to-propane ratio for partial oxidation is readily seen to be 1.5, however, as evidenced from the experimental results, this ratio does not correspond to the ideal value for fuel cell power output, which instead falls within the range 3–4 for the temperatures examined. There is a complex interplay between anode chemical catalysis, anode electrocatalysis, cathode electrocatalysis, and gas transport between electrodes that establishes the ideal gas composition for any given temperature, and a complete evaluation of all relevant processes, which also depend on structural details such as electrode thickness, porosity, average pore size, pore size distribution, fuel cell dimensions, gas flow pattern, etc. [5], is beyond the scope of the present work. An example of the complexity is embodied in the observation presented in Fig. 5 that the open circuit voltage increases with increasing oxygen flow rate. Thermodynamic calculations in which it is assumed that the anode yields an equilibrium gas composition and that the cathode retains the inlet gas composition indicate that the OCV should instead decrease monotonically within increasing O_2/C_3H_8 [18]. In addition, the increase in temperature due to the higher gas flow rate (see Fig. 7) would be expected to also reduce the voltage due to increasing electronic conductivity of the SDC electrolyte [29]. This contradiction leads us to suggest that the CO and H_2 yields from oxidation over nickel deviate substantially from the thermodynamic values and may be enhanced under higher gas flow rates.

In terms of the functionality of $Bi_2V_{0.9}Cu_{0.1}O_{5.35}$-based single-chamber fuel cells, it is apparent that this material has drawbacks relative to alternatives such as $(Ba_{0.5}Sr_{0.5})(Co_{0.8}Fe_{0.2})O_{3-\delta}$ [4,6] and $(Sm_{0.5}Sr_{0.5})CoO_{3-\delta}$ [18]. While the open circuit voltage is comparable to cells based on those other materials, indicating the benefits of the low activity for chemical combustion of propane, the polarization curves display steep slopes, suggesting that $Bi_2V_{0.9}Cu_{0.1}O_{5.35}$ may be rather ineffective for electrochemical reduction of oxygen. Furthermore, the microstructural stability of the cathode material is attained only when the gas stream temperatures are low enough to keep the fuel cell temperature below 600°C. Given the local heating effects due to partial oxidation, such conditions are met only when the gas stream temperature is well below 600°C (by 70–100°C). At low temperatures, however, carbon deposition can become problematic, particularly at lower oxygen-to-propane ratios. Balancing these requirements must further be achieved while balancing the optimal gas flow conditions for fuel cell power output, which, in turn, feed back into the heat release effects and thereby the fuel cell temperatures. Consequently, $Bi_2V_{0.9}Cu_{0.1}O_{5.35}$-based single-chamber solid-oxide fuel cells running on propane are operable only in a very narrow range of temperatures, oxygen-to-propane ratios, and total gas flow rates. While optimization of gas-phase composition and thermal management of propane fueled SCFCs is difficult even for the more active cathode materials, the challenges are particularly severe here because conditions that lead to local temperature rises at the fuel cell are highly detrimental to $Bi_2V_{0.9}Cu_{0.1}O_{5.35}$ structural stability. Thus, although $Bi_2V_{0.9}Cu_{0.1}O_{5.35}$ shows some promising characteristics for single-chamber SOFC operation such as good stability under relatively high propane partial pressures, low activity for propane chemical oxidation, and low reactivity with SDC, the difficulties in maintaining fuel cell conditions such that high power output is achieved without inducing temperature rises that cause structural degradation of $Bi_2V_{0.9}Cu_{0.1}O_{5.35}$ discourage further consideration of this material for SC-SOFC applications.

Acknowledgment

This work was funded by DARPA, Microsystems Technology Office under Award No. N66001-01-1-8966. Additional support was provided by the National Science Foundation, Division of Materials Research, through its support of the Caltech Center for the Science and Engineering of Materials under Grant No. DMR-0520565.

References

[1] Hibino, T., Hashimoto, A., Inoue, T., Tokuno, J., Yoshida, S., and Sano, M., 2000, "A Low-Operating-Temperature Solid Oxide Fuel Cell in Hydrocarbon-Air Mixtures," Science, **288**, pp. 2031–2033.

[2] Dyer, C. K., 1990, "A Novel Thin-Film Electrochemical Device for Energy Conversion," Nature (London), **343**, pp. 547–548.

[3] Yano, M., Tomita, A., Sano, M., and Hibino, T., 2007, "Recent Advances in Single-Chamber Solid Oxide Fuel Cells: A Review," Solid State Ionics, **177**, pp. 3351–3359.

[4] Shao, Z. P., Haile, S. M., Ahn, J., Ronney, P. D., Zhan, Z. L., and Barnett, S. A., 2005, "A Thermally Self-Sustained Micro Solid-Oxide Fuel-Cell Stack With High Power Density," Nature (London), **435**, pp. 795–798.

[5] Hao, Y., Shao, Z. P., Mederos, J., Lai, W., Goodwin, D. G., and Haile, S. M., 2006, "Recent Advances in Single-Chamber Fuel-Cells: Experiment and Modeling," Solid State Ionics, **177**, pp. 2013–2021.

[6] Shao, Z. P., and Haile, S. M., 2004, "A High-Performance Cathode for the Next Generation of Solid-Oxide Fuel Cells," Nature (London), **431**, pp. 170–173.

[7] Shao, Z. P., Mederos, J., Chueh, W. C., and Haile, S. M., 2006, "High Power-Density Single-Chamber Fuel Cells Operated on Methane," J. Power Sources, **162**, pp. 589–596.

[8] Aurivillius, B., 1951, "Mixed Oxides With Layer Lattices. 3. Structure of $BaBi_4Ti_4O_{15}$," Ark. Kemi, **2**, pp. 519–527.

[9] Aurivillius, B., 1950, "Mixed Bismuth Oxides With Layer Lattices. 2. Structure of $Bi_4Ti_3O_{12}$," Ark. Kemi, **1**, pp. 499–512.

[10] Aurivillius, B., 1950, "Mixed Bismuth Oxides With Layer Lattices. 1. The Structure Type of $CaNb_2Bi_2O_9$," Ark. Kemi, **1**, pp. 463–480.

[11] Abraham, F., Debreuille-Gresse, M. F., Mairesse, G., and Nowogrocki, G., 1988, "Phase Transitions and Ionic Conductivity in $Bi_4V_2O_{11}$ an Oxide With a Layered Structure," Solid State Ionics, **28–30**, pp. 529–532.

[12] Kendall, K. R., Navas, C., Thomas, J. K., and Zurloye, H. C., 1996, "Recent Developments in Oxide Ion Conductors: Aurivillius Phases," Chem. Mater., **8**, pp. 642–649.

[13] Abraham, F., Boivin, J. C., Mairesse, G., and Nowogrocki, G., 1990, "The Bimevox Series: A New Family of High Performances Oxide Ion Conductors," Solid State Ionics, **40–41**, pp. 934–937.

[14] Boivin, J. C., and Mairesse, G., 1998, "Recent Material Developments in Fast Oxide Ion Conductors," Chem. Mater., **10**, pp. 2870–2888.

[15] Goodenough, J. B., Manthiram, A., Paranthaman, P., and Zhen, Y. S., 1992, "Fast Oxide-Ion Conduction in Intergrowth Structures," Solid State Ionics, **52**, pp. 105–109.

[16] Xia, C. R., and Liu, M. L., 2002, "Novel Cathodes for Low-Temperature Solid Oxide Fuel Cells," Adv. Mater. (Weinheim, Ger.), **14**, pp. 521–523.

[17] Shao, Z. P., Yang, W. S., Cong, Y., Dong, H., Tong, J. H., and Xiong, G. X., 2000, "Investigation of the Permeation Behavior and Stability of a $Ba_{0.5}Sr_{0.5}Co_{0.8}Fe_{0.2}O_{3-\delta}$ Oxygen Membrane," J. Membr. Sci., **172**, pp. 177–188.

[18] Shao, Z. P., Kwak, C., and Haile, S. M., 2004, "Anode-Supported Thin-Film Fuel Cells Operated in a Single Chamber Configuration 2T-I-12," Solid State Ionics, **175**, pp. 39–46.

[19] Watanabe, A., and Das, K., 2002, "Time-Dependent Degradation Due to the Gradual Phase Change in BICUVOX and BICOVOX Oxide-Ion Conductors at Temperatures Below About 500°C," J. Solid State Chem., **163**, pp. 224–230.

[20] Dygas, J. R., Kurek, P., and Breiter, M. W., 1995, "Structure-Dependent Impedance of BICUVOX," Electrochim. Acta, **40**, pp. 1545–1550.

[21] Watanabe, A., 1997, "$Bi_{23}M_4O_{44.5}$ (M=P and V): New Oxide-Ion Conductors With Triclinic Structure Based on a Pseudo-Fcc Subcell," Solid State Ionics, **96**, pp. 75–81.

[22] Watanabe, A., 2001, "Preparation and Characterization of a New Triclinic Compound $Bi_{3.5}V_{1.2}O_{8.25}$ to Show the Known Phase $Bi_4V_2O_{11}$ to be Nonexistent as a Single Phase," J. Solid State Chem., **161**, pp. 410–415.

[23] Pang, G. S., Feng, S. H., Tang, Y. C., Tan, C. H., and Xu, R. R., 1998, "Hydrothermal Synthesis, Characterization, and Ionic Conductivity of Vanadium-Stabilized $Bi_{17}V_3O_{33}$ With Fluorite-Related Superlattice," Chem. Mater., **10**, pp. 2446–2449.

[24] Wrobel, W., Krok, F., Abrahams, I., Kozanecka-Szmigiel, A., Malys, M., Chan, S. C. M., and Dygas, J. R., 2006, "$Bi_8V_2O_{17}$ – a Stable Phase in the Bi_2O_3-V_2O_5 System," Mater. Sci. (Poland), **24**, pp. 23–30.

[25] Mauvy, F., Launay, J. C., and Darriet, J., 2005, "Synthesis, Crystal Structures and Ionic Conductivities of $Bi_{14}P_4O_{31}$ and $Bi_{50}V_4O_{85}$. Two Members of the Series $Bi_{18-4m}M_{4m}O_{27+4m}$ (M=P, V) Related to the Fluorite-Type Structure," J. Solid State Chem., **178**, pp. 2015–2023.

[26] Turkoglu, O., and Belenli, I., 2003, "Electrical Conductivity of γ-Bi_2O_3-V_2O_5 Solid Solution," J. Therm Anal. Calorim., **73**, pp. 1001–1012.

[27] Watanabe, A., 2000, "Highly Conductive Oxides, $CeVO_4$, $Ce_{1-x}M_xVO_{4-0.5x}$ (M=Ca, Sr, Pb) and $Ce_{1-y}Bi_yVO_4$, With Zircon-Type Structure Prepared by Solid-State Reaction in Air," J. Solid State Chem., **153**, pp. 174–179.

[28] Hibino, T., Hashimoto, A., Inoue, T., Tokuno, J., Yoshida, S., and Sano, M., 2001, "A Solid Oxide Fuel Cell Using an Exothermic Reaction as the Heat Source," J. Electrochem. Soc., **148**, pp. A544–A549.

[29] Inaba, H., and Tagawa, H., 1996, "Ceria-Based Solid Electrolytes," Solid State Ionics, **83**, pp. 1–16.